Journal of Materials Processing Tech. 251 (2018) 305–316

Contents lists available at ScienceDirect

Journal of Materials Processing Tech.

journal homepage: www.elsevier.com/locate/jmatprotec

Research Paper

Effect of welding parameters and B_4C contents on the microstructure and mechanical properties of friction stir welded B_4C/6061Al joints

Y.Z. Li[a,1], Q.Z. Wang[a,*], B.L. Xiao[b], Z.Y. Ma[b,*]

[a] Key Laboratory of Nuclear Materials and Safety Assessment, Institute of Metal Research, Chinese Academy of Sciences,72 Wenhua Road, Shenyang 110016, China
[b] Shenyang National Laboratory for Materials Science, Institute of Metal Research, Chinese Academy of Sciences,72 Wenhua Road, Shenyang 110016, China

ARTICLE INFO

Keywords:
B_4C
Friction stir welding
Composites
Microstructure
Mechanical property

ABSTRACT

Annealed 2.8 mm thick B_4C/6061Al composite sheets with various B_4C particle contents (15, 20, 25, 30 wt%) were friction stir welded (FSW) at a tool rotation rate of 1000 rpm and traverse speeds of 50 and 150 mm/min using a single simple-shaped wear-resistant cermet tool. Sound FSW joints were obtained without severe abrasion of the tool. FSW resulted in obvious homogenization and fragmentation of B_4C and the re-distribution of the interfacial products, thereby remarkably increased the hardness of the nugget zone. The hardness profiles of the welded joints were hardly influenced by B_4C contents but significantly by the welding speeds. "S" line and a B_4C depleted region were formed at the top and the bottom of the nugget zone, respectively. However, they did not deteriorate the mechanical properties of the joints. The tensile strength of all the joints was close or even up to that of the base material with the fracture occurring at the base material.

1. Introduction

Particle reinforced aluminum matrix composites (PRAMCs) have received significant attentions for aerospace and automotive applications (Clyne and Withers, 1993; Lloyd, 1994), but the poor weldability constraints the wide application of PRAMCs. Ellis (1996) reported that it is very difficult to achieve perfect welding of PRAMCs by means of diffusion welding because of the huge difference between the reinforcement and the matrix alloy. Different welding methods have been employed to weld PRAMCs, such as pulse laser by Dahotre et al. (1991) and friction stir welding (FSW) by Nelson et al. (2000). Among these methods, FSW was proven, by Mishra and Ma (2005) and Wang et al. (2014a), to be a promising method for welding the PRAMCs due to the avoidance of the drawbacks in fusion welding.

However, there were still some key challenges that must be faced in the FSW of PRAMCs. Firstly, Feng and Ma (2007), Feng et al. (2008) found that the existence of ultrahard reinforcements in PRAMCs led to severe wear of the steel tool during FSW. This not only results in the difficulty in realizing the long distance welding, but also deteriorates the properties of the FSW joints. Secondly, the much lower plasticity of PRAMCs limited the choice of the welding parameters and easily led to the formation of the welding defects. Recently, Wang et al. (2014b,c) reported that sound joints of PRAMCs were obtained by FSW, but only for the composites with lower reinforcement content.

As a new kind of reinforcement, B_4C has lower density (about 2.52 g/cm^3) and higher hardness (9.5+ in Mohs' scale) among ultrahard materials (Lee et al., 2001). Viala et al. (1997) considered B_4C particle as an alternative to SiC and Al_2O_3 particles for fabricating advanced PRAMCs with high stiffness, wear resistance and impact resistance combining with similar thermal stability and chemical inertness. Especially, the specific ability of the B-10 isotope to capture neutrons makes B_4C particle reinforced Al composite (B_4Cp/Al) become an ideal neutron absorbing material in the storage and transportation of spent nuclear fuel (Abenojar et al., 2007; Kang et al., 2010). For this application, welded structures of B_4Cp/Al are required, especially for the B_4Cp/Al with higher B_4C content to obtain higher neutron absorbing ability.

However, the challenges in FSW of the B_4Cp/Al are even tougher for higher hardness of B_4Cp. The investigations on FSW of the B_4Cp/Al are still limited so far. Nelson et al. (2000) used a steel pin to weld the (15–30) wt% B_4Cp/6061Al and found that the screw thread was almost completely eliminated for a welding distance of only 254 mm and a great amount of tool debris was detected in the joint. Kalaiselvan and Murugan (2013a,b), Kalaiselvan et al. (2014) used a quadrangular steel pin to weld the (4–12) wt% B_4Cp/6061Al with a maximum welding speed of 140 mm/min. It was reported that the tunnel-like defects were observed at most welding parameters. Guo et al. (2012) and Chen et al. (2009) used a taper pin to weld the B_4Cp/1100Al with 16 and 30 vol.%

* Corresponding authors.
E-mail addresses: yuze.li@im2np.fr (Y.Z. Li), qzhwang@imr.ac.cn (Q.Z. Wang), zyma@imr.ac.cn (Z.Y. Ma).
[1] Now is with Aix-Marseille University, CNRS, IM2NP UMR 7334, 13397, Marseille, France.

http://dx.doi.org/10.1016/j.jmatprotec.2017.08.028
Received 23 November 2016; Received in revised form 19 August 2017; Accepted 19 August 2017
Available online 01 September 2017
0924-0136/

B_4Cp, and the B_4Cp/6063Al with 6 and 10.5 vol.% B_4Cp. The tool wear was alleviated due to the simple tool shape, and a relatively higher joint efficiency was obtained. From these studies, it can be concluded that low B_4Cp contents, low composite strength, and simple shape of welding tool were beneficial to avoiding the severe tool wear in FSW of the B_4Cp/Al.

The simple-shaped welding tool not only could alleviate the tool wear but also facilitates to the manufacture of welding tool when a high wear resistance material is used. However, the simple-shaped tool is not beneficial to inducing the flow of material during FSW, in which case the defects may be easily generated. Moreover, for the B_4Cp/Al with higher B_4Cp content, sound welding is still a severe challenge by using the simple-shaped welding tool due to very low plasticity of the composites.

In this study, a new wear-resistant cermet pin with a simple shape (tri-prism, without thread) was used for FSW of the B_4Cp/6061Al with 15–30 wt% B_4Cp at two welding speeds. The aim is (a) to verify the feasibility of conducting multi-pass welding to achieve the perfect FSW joints using a single simple-shaped welding tool and (b) to understand the effect of the welding parameters and the B_4Cp contents on the microstructural evolution and the mechanical properties of FSW joints.

2. Experimental

The B_4Cp/6061Al composites with the B_4Cp weight fractions of 15, 20, 25 and 30% were fabricated by a powder metallurgy (P/M) technique, using 6061Al alloy with a nominal composition of Al-1.0Mg-0.65Si-0.25Cu (wt%) as the matrix and 7 μm B_4Cp as the reinforcement. The fabrication process of the composites has been described in detail in our previous study (Li et al., 2015a). The composite billets 350 mm in diameter were hot-pressed at 620 °C for 120 min, hot-extruded into planks, and then hot-rolled to sheets 2.8 mm in thickness, which is a typical thickness for the storage and transportation of spent nuclear fuel.

The sheets with a length of 300 mm and a width of 75 mm were butt-welded along the rolling direction using a FSW machine. Based on previous reports (Feng et al., 2008) and our welding trials, a rotation rate of 1000 rpm and welding speeds of 50 and 150 mm/min were selected as the welding parameters in this study. A tool with a shoulder 14 mm in diameter and a tri-prism pin 5 mm in root diameter was made of TiC reinforced Ni cermet. A single tool was used for the welding of all the composite samples under various FSW parameters with an accumulative total welding distance of ~1200 mm. The FSW samples were designated using a series digital format in Table 1. For example, sample 15–50 denotes that the B_4Cp content of the sample was 15 wt% and the welding speed was 50 mm/min.

Because B_4Cp/6061Al composite is used as neutron absorbing material and the mechanical strength is not the main concerns, the composite sheets were completely annealed (400 °C for 150 min, furnace-cooled) before FSW in orde to reduce the hardness of the composite, thereby modifying the formability of the welds and reducing the tool wear.

After welding, the FSW samples were cross-sectioned perpendicular to the welding direction for microstructural examinations by optical microscopy (OM) and scanning electron microscopy (SEM, quanta 600). Metallographic specimens were mechanically polished to a colloidal 50 nm SiO_2 finish and then etched by Keller's reagent. The phase analyses of the base metal (BM) and the nugget zone (NZ), of the 15–50 and 20–50 joints as the representatives, were conducted using an X-ray diffraction (XRD) analyzer (D/max 2400) with the X-ray wavelength of 1.5406 Å, the aperture size of 10 mm × 1 mm and the step size of 0.04°/s. The data was processed with MDI Jade 5.0. The interface microstructures of the BM and the NZ, of the 20–50 joint as a representative, were examined by transmission electron microscopy (TEM, TECNAI G2 F20), operating at 200 kV. The thin foils for TEM were prepared by ion-milling technique. Both the analysis surfaces for XRD and TEM were parallel to the sheet surface.

The Vickers hardness profiles of the joints were measured on the cross-sections perpendicular to the welding direction, using a Vickers hardness tester under a 1000 gf load for 30 s. Dog-bone-shaped tensile specimens with a gauge length of 40 mm and a width of 10 mm were machined perpendicular to the welding direction with the NZ being in the center of the gauge. Room-temperature tensile tests were carried out at a strain rate of $1 \times 10^{-3}\,s^{-1}$ and the property data for each condition was obtained by averaging three testing results. The fracture surfaces of the tensile specimens were observed under an SEM.

Table 1
Designations of FSW B_4Cp/6061Al samples.

Samples	Particle content, wt%	Welding speed (υ), mm/min	Designation
1	15	50	15–50
2	15	150	15–150
3	20	50	20–50
4	20	150	20–150
5	25	50	25–50
6	25	150	25–150
7	30	50	30–50
8	30	150	30–150

3. Results

3.1. Macroscopic morphologies of the tool and welded joints

Fig. 1 shows the macroscopic morphologies of the welding tool before and after welding all the B_4Cp/6061Al samples with various B_4Cp contents under investigated FSW parameters. Obvious abrasion of the pin was observed after about 1200 mm of welding distance, as shown in Fig. 1. However, almost all the abrasion occurred at the ridge of the pin, the head face and the edge planes still maintained the original morphology, and no obvious shortening of the pin was detected. Furthermore, almost no abrasion was detected on the shoulder. This indicates that this simple-shaped cermet welding tool exhibited good wear resistance even for multi-pass welding of eight composite samples.

Fig. 2 illustrates the FSW joints of B_4Cp/6061Al composites with various B_4Cp contents and welding speeds. The surfaces of the joints were characterized by the so-called wake effect as demonstrated (Ceschini et al., 2007), with the presence of semicircular features, similar to those observed in FSW monolithic Al alloys (Cui et al., 2008). The surfaces of all the joints were smooth and no defects were detected in the joints, indicating that sound joining was achieved. The surface quality of the joints did not become worse with the increase of the B_4Cp contents and welding speeds.

3.2. Microstructure of B_4Cp/6061Al composites with various B_4Cp contents

Fig. 3 shows the cross section microstructure of the rolled B_4Cp/

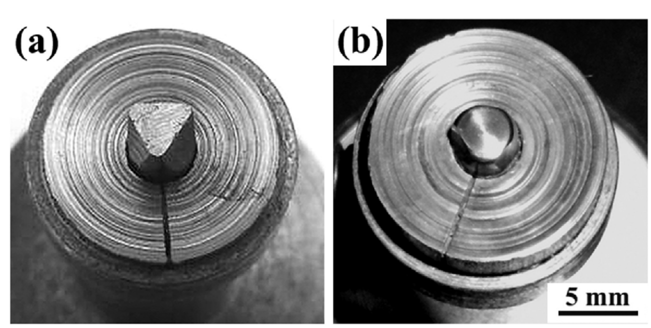

Fig. 1. The morphologies of welding tool (a) before and (b) after welding all B_4Cp/6061Al samples with a welding distance of ~1200 mm.